HYDROGEN COSTS FOR THE PBMR THERMAL REACTOR AND THE WESTINGHOUSE PROCESS

David F. McLaughlin[1], Samuel A. Paletta[1], Edward J. Lahoda[1], Willem Kriel[2], Michael M. Nigra[1], and Garrett T. McLaughlin[1]
[1]Westinghouse Electric Company, LLC, Science and Technology Department, 1344 Beulah Road, Pittsburgh, PA 15235-5083
[2]PBMR, 1344 Beulah Road, Pittsburgh, PA 15235-5083
November 2005

Executive Summary

A study of the economics for producing hydrogen from the Pebble Bed Modular Reactor (PBMR) and the Westinghouse Sulfur Process (WSP) has been carried out. These calculations used a version of the PBMR that has been designed for the production of process heat at a temperature of 700 to 950°C. Process heat is used by the WSP to perform the decomposition of the SO_3 to O_2 and SO_2. Electricity for the WSP electrolysis step that produces hydrogen is obtained either off of the grid and/or from the PBMR itself using either a Rankine or Brayton cycle.

The goal of this study was to determine the best combination of power conversion unit (PCU), intermediate heat transfer (IHX) loop fluid, and WSP electrolysis unit. Chemical process modeling was completed to analyze the many combinations of the above choices. Over sixty different configurations were evaluated using the CHEMCAD chemical process simulation software.(1) The PCU, the IHX loop from the reactor to the WSP, and the WSP itself were modeled. The results indicate that:

1. The sulfuric acid based WSP was the most efficient process (46.5% using the lower heating value of H_2 and 38% PCU efficiency).
2. The lowest cost H_2 is made by making no electrical power over that needed to run the WSP.
3. There was no significant efficiency difference between using a high pressure Rankine cycle or a Brayton cycle at the high thermal energy extractions used in a process heat PBMR configuration. Note that this conclusion changes if one PBMR is used exclusively for thermal power to the WSP and another is used exclusively for electrical generation. In this case, the Brayton cycle with 43% efficiency would definitely be preferred for the PCU.
4. The higher PBMR outlet temperatures gave slightly higher overall WSP and PCU efficiencies.
5. Though there is a large relative difference between the energy costs of the molten salt and He high temperature heat transfer loops, the efficiency differences are small in relation to the overall energy balance. Therefore, the approach that leads to the most convenient design and operation should be followed.

The combination of the current aqueous sulfuric acid approach for the WSP which had the highest overall energy efficiency when tied to the PBMR with:

1. 600 MWt PBMR with a 950°C outlet;

2. Either a high pressure (18 MPa) steam Rankine cycle or an 8.6 MPa Brayton cycle (both efficiencies of ~38%) for the PCU;
3. 44% split between thermal power to the WSP and 56% to the PCU cycle;
4. Either molten salt or He high temperature heat transfer loop;
5. The aqueous H_2SO_4 variant of the WSP operating at 5 to 10 MPa pressure.

The options were evaluated economically assuming the cost of electrical power at $35/MWh(e) and cost of PBMR thermal power at $15 MWh(t), giving energy costs of $0.99/kg H_2. Capital and O&M costs add about $0.67/kg H_2, so that the overall process produces hydrogen at a cost of about $1.67/kg of H_2.

1. Introduction

The Westinghouse Sulfur Process (WSP) uses thermal and electrical energy from a Pebble Bed Modular Reactor (PBMR) to produce hydrogen. Helium is used as the reactor coolant, which after leaving the nuclear reactor goes through an intermediate heat exchange loop (IHX). Here heat is transferred from the reactor helium to a heat transfer fluid (either He or molten salt) that carries the process heat from the PBMR to the physically isolated WSP plant where it is used in the SO_3 decomposition reactor. After the IHX, the reactor helium enters the Power Conversion Unit (PCU), either a Brayton or Rankine cycle, which produces power to run the electrolyzer for the WSP. Any remaining power sold to the grid. Figure 1 shows the connections between the different parts of the overall model.

Each of the three major portions, PCU, IHX, and WSP, was modeled separately. The PCU Brayton cycle with no heat removed to the IHX was benchmarked against the existing PBMR data to ensure that the PCU process model was accurate. The IHX and WSP

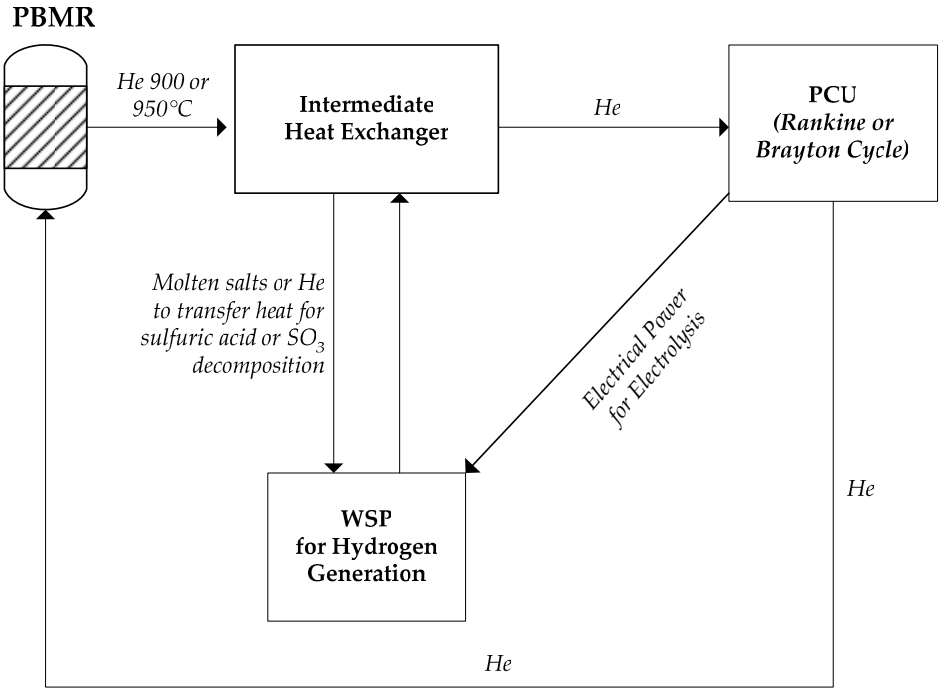

Figure 1 - Connection of the PBMR to the IHX and WSP

processes were decoupled and then evaluated and benchmarked against the coupled models for the IHX and WSP. It was determined that the IHX and WSP could be decoupled if the parameters for the WSP were set from the thermal power and reactor temperature values determined from the integrated IHX-WSP model.

2. Power Conversion Unit Modeling

Both the Brayton cycle and Rankine cycles were included in models for power generation cycles along with the WSP for hydrogen generation. Varying amounts of thermal power (0, 50, 100, and 150 MWt) were sent to the intermediate heat exchange system and the remainder of thermal power was sent to the PCU to be converted to electrical power. The Brayton cycle uses the hot helium in the reactor loop directly while the Rankine cycle transfers power through a secondary helium loop to produce steam. Table 1 shows the temperature of the helium leaving the reactor and output temperatures for the models along with the total thermal power extracted. Two different Rankine cycles were analyzed (low and high pressure steam), both with an intermediate loop to isolate primary reactor He from water.

Table 1 - Power Cycle Parameters

Total PBMR Thermal Power	Reactor Outlet He Temperature	Reactor Return He Temperature
600 MWt	900°C	300°C
600 MWt	950°C	350°C
400 MWt	900°C	500°C
450 MWt	950°C	500°C

2.1 Brayton Cycle Analysis

The Brayton cycle uses the helium directly from the reactor to drive gas turbines to produce power. In the current design, the PBMR uses one power turbine and two compressors on one shaft.[2] For the modeling purposes, a Brayton cycle with three turbines and two compressors was used and shown in benchmark calculations to be comparable to a one-turbine, two-compressor Brayton cycle in the current flow sheet of the plant. The three–turbine/two-compressor model is shown in Figure 2. Energy needed for the WSP is removed from the helium by the IHX. After the heat is removed by the intermediate loop, the helium then enters the turbines in the Brayton cycle. Both high pressure turbines (HPT) and low pressure turbines (LPT) have a assumed efficiencies of 92%. The third power turbine (PT) has an efficiency of 91.5%. All three turbines were modeled as adiabatic machines. In the recuperator following the turbine system, an assumed temperature difference of 50°C is maintained between the output temperature of the turbine and the output temperature on the high pressure side of the recuperator. It should be noted that after the high pressure compressor, some of the flow is removed as a “leak flow,” to cool the blade roots and the blade disks (although there is no blade cooling). The leak flow is removed after the second (high pressure) compressor and returned back to the system directly before the recuperator.[3] All of the models were run with a primary PBMR helium flowrate of 185 kg/s.[4]

The efficiencies and net power of the Brayton cycle for each of models in Table 1 were determined. From this analysis, it was found that the highest efficiency Brayton cycles are

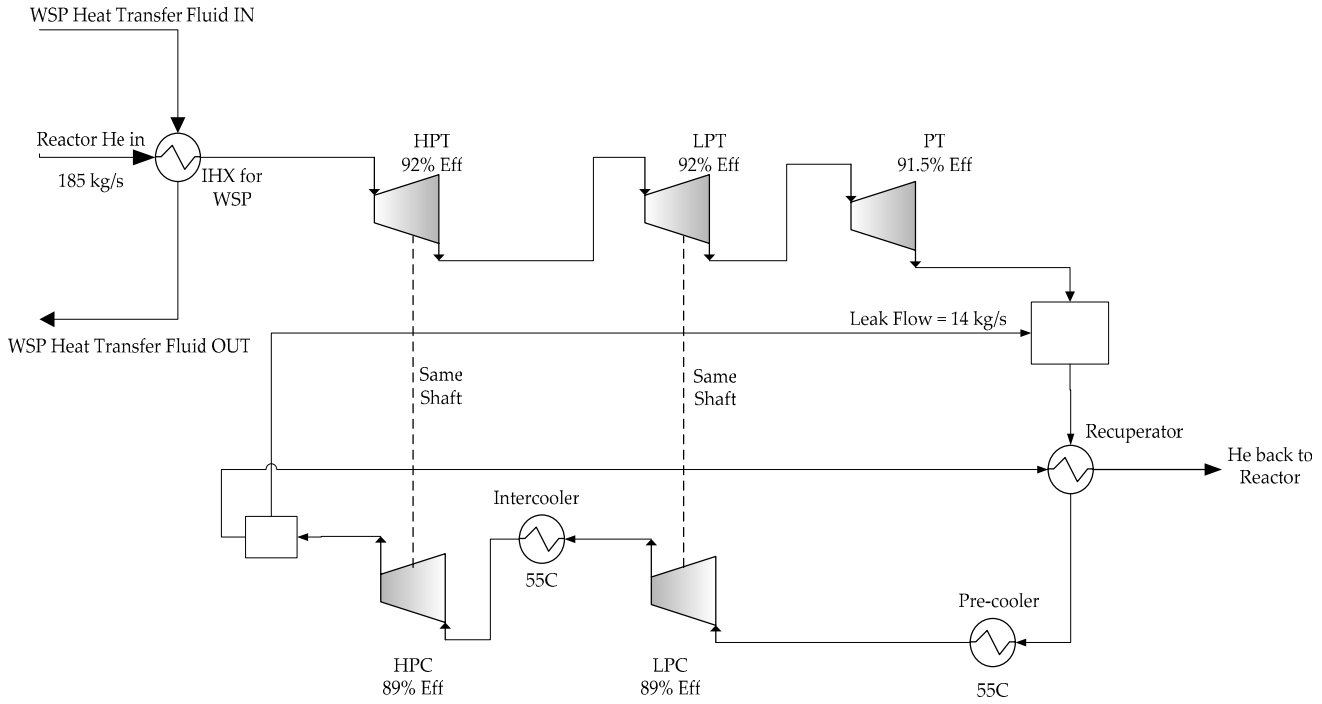

Figure 2 - Brayton Cycle Flowsheet

found for the 400 and 450 MWt cases when 0 MW is removed to the IHX. As seen in Table 2, the 400 and 450 MWt cases have higher efficiencies than their 600 MWt counterparts. The decrease in efficiency was due to the higher low-pressure compressor (LPC) powers for the 600 MWt models than the 400/450 MWt models. (The powers for the HPC were all the same because they all enter and leave at the same temperature and pressure after the intercooler).

2.2 Rankine Cycle Analysis

In contrast to the Brayton cycle, the Rankine cycle does not produce power directly from the reactor helium. The Rankine cycle transfers thermal energy using a secondary helium exchange (SHX) loop to transfer power to the Rankine cycle to make steam; this design ensures that under no conditions can water infiltrate the reactor primary system and cause unwanted moderation in the reactor core. Steam then goes through the power generating turbines. The flowsheet for a Rankine cycle with an SHX loop is shown in Figure 3.

A primary helium mass flow of 185 kg/s was again assumed for all cases, the same as for the Brayton cycle models. As with the Brayton cycle models, the energy consumed by the WSP is removed first from the primary He in the IHX. The energy for the Rankine cycle is then removed from the primary helium with the secondary helium heat exchanger. Secondary helium leaves the IHX 50°C cooler than the primary helium temperature entering the IHX. The pressure drop through the heat exchange loop heat exchangers is assumed to be the same as that through the recuperator of the Brayton cycle.

The flow rate of the water feed was adjusted for each of the models to give a constant He flow and a set ΔT for the helium. Starting with preheater 2 in Figure 3, the output

Table 2 – Brayton Cycle Efficiency and z_{PCU} vs. PBMR and WSP Power Levels

P_{PBMR} (MWt)	He Inlet T(°C)	He Outlet T(°C)	P_{WSP} (MWt)	$P_{Turbine}$ (MWe)	$\eta = P_{Turbine}/(P_{PBMR}-P_{WSP})$	$z_{PCU} = P_{Turbine}/P_{PBMR}$
577.3	900	300	0	175.4	0.303	0.301
			50	158.9	0.302	0.273
			100	142.1	0.298	0.244
			150	124.8	0.292	0.214
577.3	950	350	0	201.7	0.349	0.346
			50	182.6	0.346	0.313
			100	163.0	0.342	0.280
			150	143.1	0.335	0.245
385.2	900	500	0	161.6	0.420	0.416
			50	135.5	0.405	0.349
			100	109.1	0.383	0.281
			150	82.5	0.352	0.212
433.1	950	500	0	186.6	0.431	0.427
			50	160.7	0.420	0.368
			100	134.5	0.404	0.308
			150	108.1	0.382	0.247

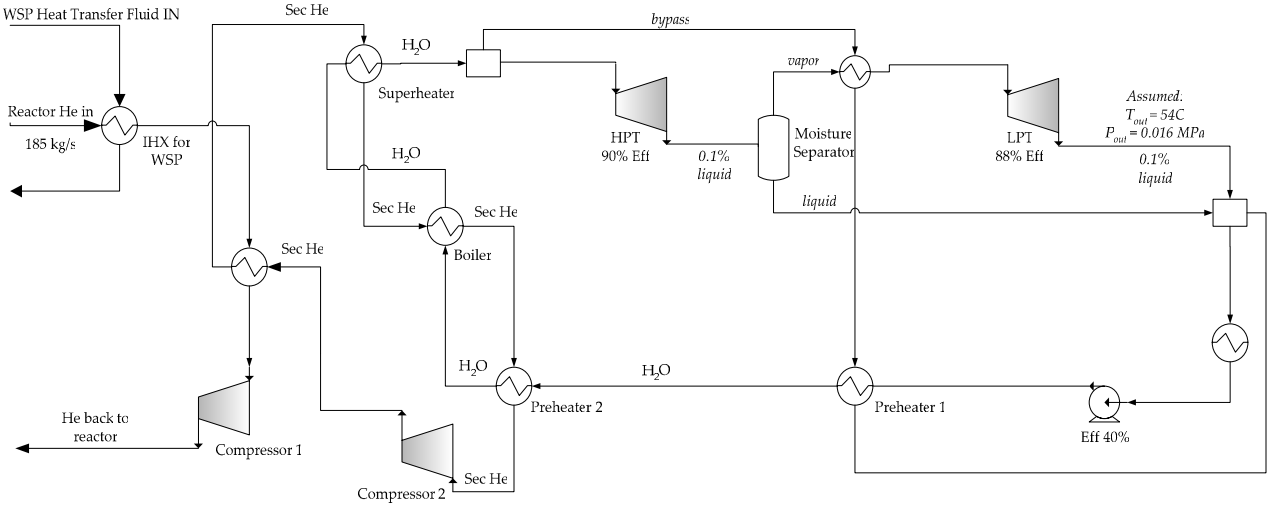

Figure 3 – Rankine Cycle Flowsheet with Secondary Helium Loop

temperature of the water is specified to be about 10°C cooler than the saturation point. In the boiler, the steam output temperature is taken to be just above saturation. The superheater is specified to have at 50°C ΔT between the hot He and the output superheated steam.

After the superheater, a small amount of steam bypassed the HPT to warm the output of the HPT in the reheater. The amount of steam that is sent to the bypass is determined so that the output temperature of the LPT is equal to 55°C. The reheater has an output vapor fraction on the bypassed steam side of 10^{-5} to fix it as saturated liquid. The HPT runs at an efficiency of 90%. The LPT has a specified output of 55°C and 0.015 MPa with an efficiency of 88%. The output of the LPT mixes with the liquid removed by the moisture separator before

going into the condenser, from which it is pumped back to the pressure at which it entered the heaters.

The Rankine cycle was evaluated at two HPT steam inlet pressures (8.6 and 18 MPa) The high-pressure Rankine cycle has a higher efficiency than the low-pressure Rankine cycle, as shown in Tables 3 and 4 which summarize the cycle and PCU efficiencies for the various cases considered. There was only about a 1-2% difference in efficiency between the two models.

2.3 Comparison of PCU Options

The three different PCU models were compared at different levels of power extraction. Up to 150 MWt extraction by the IHX, the Brayton cycle run with a return temperature at around 500°C generally has the best efficiency. Above about 150 MWt to the WSP or for very low primary He return temperatures (300°C and 350°C), the high temperature-pressure Rankine cycle was the most efficient. Note that for low return temperatures, the low pressure Rankine cycle was still more efficient than the Brayton cycle.

3. Intermediate Heat Transfer Loop Modeling

3.1 Flowsheet

The physical separation of the PBMR from the hydrogen generation plant requires a long heat transfer pipeline. A separation distance of 400 meters was chosen to evaluate the

Table 3 – High Pressure (18 MPa) Rankine Cycle Efficiency and z_{PCU} versus PBMR and WSP Power Levels

P_{PBMR} (MWt)	He Inlet T(°C)	He Outlet T (°C)	P_{WSP} (MWt)	$P_{Turbine}$ (MWe)	$\eta = P_{Turbine}/(P_{PBMR}-P_{WSP})$	$z_{PCU} = P_{Turbine}/P_{PBMR}$
577.3	900	300	0	230.6	0.400	0.395
			50	206.6	0.392	0.354
			100	183.2	0.384	0.314
			150	160.3	0.375	0.275
577.3	950	350	0	233.2	0.404	0.400
			50	209.7	0.398	0.360
			100	186.1	0.390	0.319
			150	163.1	0.382	0.280
385.2	900	500	0	151.3	0.393	0.389
			50	130.0	0.388	0.334
			100	108.0	0.379	0.278
			150	86.7	0.369	0.223
433.1	950	500	0	173.2	0.400	0.396
			50	151.3	0.395	0.346
			100	128.7	0.386	0.294
			150	106.8	0.377	0.244

Table 4 – Low Pressure (8.6 MPa) Rankine Cycle Efficiency and z_{PCU} versus PBMR and WSP Power Levels

P_{PBMR} (MWt)	He Inlet T(°C)	He Outlet T (°C)	P_{WSP} (MWt)	$P_{Turbine}$ (MWe)	$\eta = P_{Turbine}/(P_{PBMR}-P_{WSP})$	$z_{PCU} = P_{Turbine}/P_{PBMR}$
577.3	900	300	0	219.2	0.380	0.376
			50	196.3	0.372	0.337
			100	174.0	0.365	0.298
			150	152.4	0.357	0.261
577.3	950	350	0	222.1	0.385	0.381
			50	199.3	0.378	0.342
			100	176.7	0.370	0.303
			150	154.8	0.362	0.266
385.2	900	500	0	145.0	0.376	0.373
			50	123.5	0.368	0.317
			100	102.6	0.360	0.264
			150	82.4	0.350	0.212
433.1	950	500	0	166.2	0.384	0.380
			50	143.7	0.375	0.329
			100	122.2	0.367	0.279
			150	101.4	0.358	0.232

heat and pumping or compressive losses. A basic schematic of this pipeline is shown in Figure 4.

In the CHEMCAD simulation of the intermediate heat exchanger unit, the mass flow rate of the heat transfer fluid is adjusted until the output temperature is equal to the desired value for the three selected parametric heat duties (50, 100 or 150 MWt). The values for the temperatures are taken to be 50°C cooler than the primary helium inlet to avoid pinch and excessive IHX surface area requirements. The heated fluid is then passed through the first of two 400 meter long "Pipe" simulators, which models frictional resistance (pressure drop) and external heat losses. The fluid then provides process heat to the WSP decomposition reactor. A compressor (for helium) or pump (for molten salt) is located between the second heat exchanger and the second pipe, returning the output pressure to the inlet pressure of the IHX

3.2 Selection of Heat Transfer Fluid

Selection of the heat transfer fluid was a key part of this analysis. Helium or a molten salt (MS) have been evaluated for use as the heat transfer fluid.[5] Many possible molten salts have been considered, including (Li,Na)F-BeF_2, (Li,Na,K)F-ZrF_4, and (Li,Na,K)F. For the current study, (46.5)LiF-(11.5)NaF-(42.0)KF was selected. Beryllium-based molten salts were eliminated due to toxicity, as well as concern about potential Be moderating capacity if there were a leak back into the reactor. The Zr salts were eliminated based on volatility concerns (normal sublimation temperature for pure ZrF_4 of 906°C) and possible HF formation if ZrF_4 makes contact with water or atmospheric moisture, leading to many safety and materials of construction issues. Properties of the (Li,Na,K)F salt were added to the CHEMCAD component database, and are listed in Table 5. Note that both fluorine and especially lithium

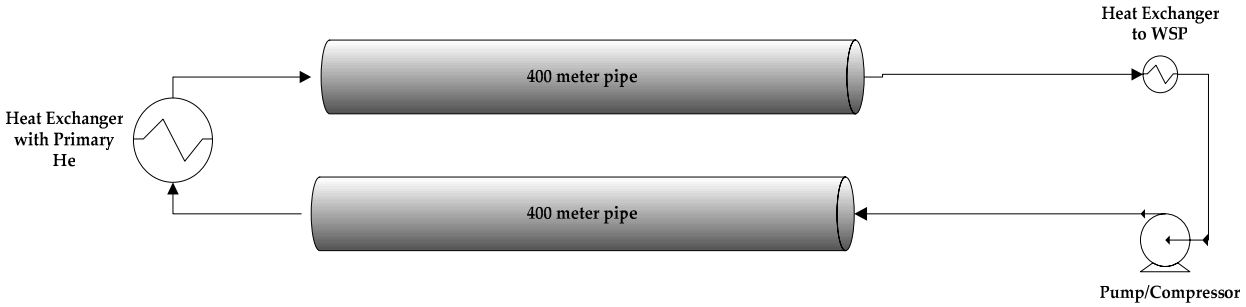

Figure 4 – Basic schematic of heat transfer pipeline

have moderating capacity as well, so that the potential nuclear reactor control implications of a leak of (Li,Na,K)F salt back into the reactor would also have to be considered in detail.

Table 5 – Properties of LiF-NaF-KF Molten Salt Heat Transfer Fluid

Composition (mol%)	MP (°C)	Cp (J/g/°C)	ρ (g/cm^3)	ρCp ($J/cm^3/°C$)	k (W/m/°C)	μ ($N\text{-}s/m^2$)
46.5-11.5-42.0	454	1.88	2.02	3.78	1.0	0.0029

3.3 Method and Results

Total circulation cost for the IHX loop includes both pumping requirements (which increase with smaller pipe diameter) and heat losses (which increase with larger pipe surface area). To find the optimum diameters for a given configuration, an IHX return temperature was selected for the fluid (He or MS), and the circulation losses were modeled for a series of different pipe diameters. For each run, the heat losses in the pipes were added to the power needed to run the compressor or pump (divided by a 38% thermal to electrical efficiency) to get a net circulation cost (MWt). This energy cost was then plotted versus pipe diameter to find the optimum pipe diameter. Figure 5 is an example of one such determination.

The minimum circulation cost at various loop fluid return temperatures was found to be a linear function of the optimum pipe diameter. From the optimum diameters, a curve was plotted of minimum circulation cost versus the return temperature for different loop delivery power values. This allows one to choose a loop temperature and to determine the optimum pipe diameter and the amount of energy lost to circulation. Results of this analysis are shown for helium (Figure 6) and the molten salt (Figure 7).

The much lower circulating costs associated with the molten salt heat transfer fluid qualify it to be looked at in more detail. The circulating costs in the IHX due to molten salts are almost negligible, whereas the circulating costs for He heat transfer fluid could reduce the efficiency of the WSP by as much at 0.5 to 1.5%. The energy savings of the MS system will be offset by operational issues, however, including corrosion, exotic pump design and materials, and issues associated with loop filling, draining, freeze prevention, and startup.

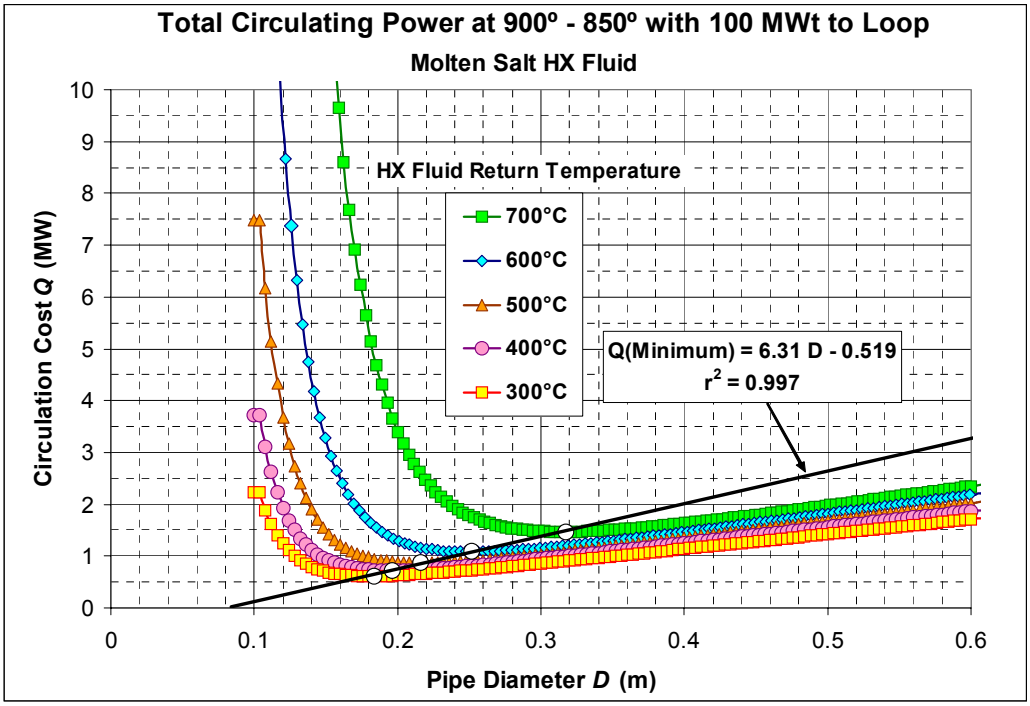

Figure 5 – Example of Optimum Intermediate Heat Transfer Loop Pipe Diameter Determination

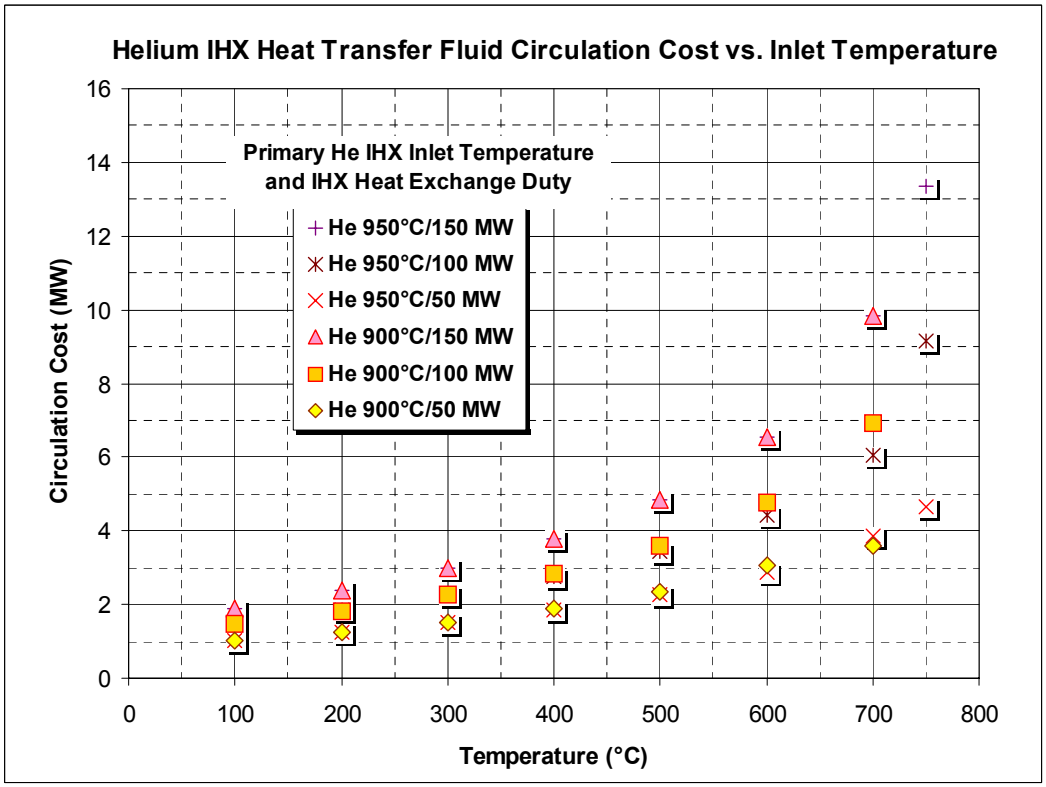

Figure 6 – Circulation Costs vs. Inlet Temperature for a Helium Intermediate Heat Exchange Loop

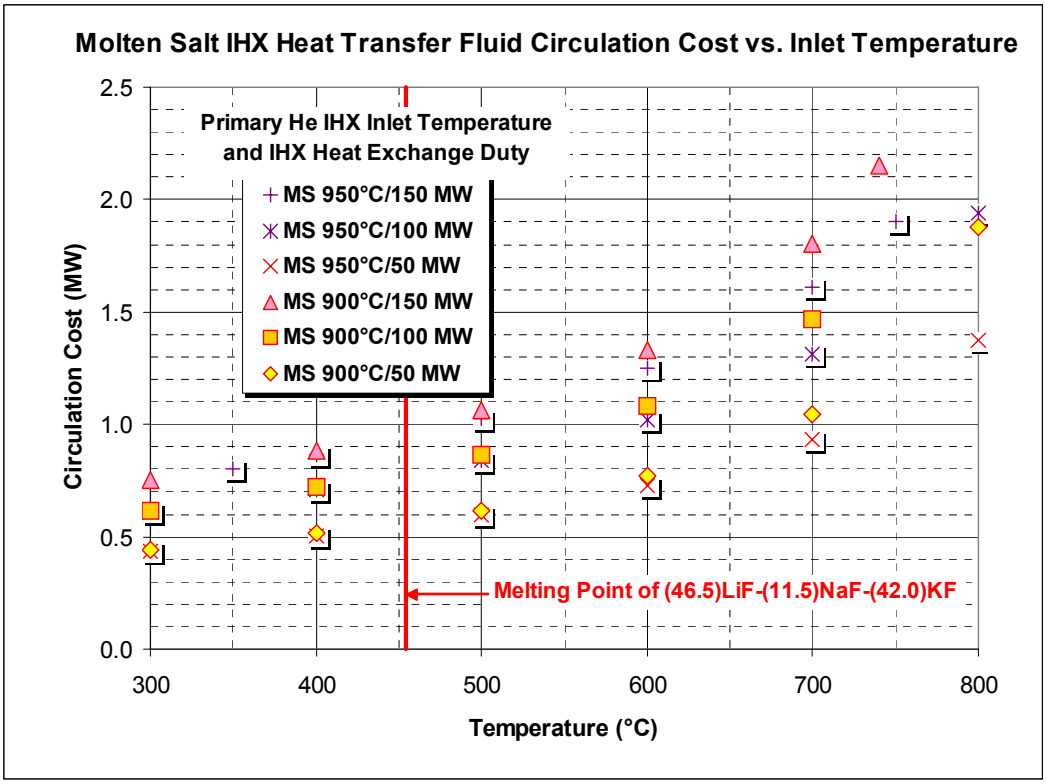

Figure 7 – Circulation Costs vs. Inlet Temperature for a Molten Salt Intermediate Heat Exchange Loop

4. The Westinghouse Sulfur Process

4.1 Overview

The Westinghouse Sulfur Process (WSP) is a hybrid process that uses both thermal energy and electrical energy to produce hydrogen. Figure 8 shows a block diagram of the WSP. The feed to the process is hexavalent sulfur, either as sulfuric acid (H_2SO_4) or sulfur trioxide (SO_3) depending on the chemistry selected for the electrolysis process. Using the thermal energy from the Intermediate Heat Exchange loop, the sulfuric acid or sulfur trioxide is thermally reduced to form tetravalent sulfur dioxide (SO_2) plus oxygen. In the case of a H_2SO_4 feed, H_2O will also be produced in the decomposition reactor. Oxygen is separated from the SO_x stream, and makeup feed water is added.

The water-SO_x mixture is then electrolyzed to generate H_2 gas. In the process, sulfur is reoxidized to S(VI), either as SO_3 or H_2SO_4. The reoxidized sulfur species is recycled back to the decomposition reactor. Thus, by generating sulfur dioxide using lower-cost thermal energy, the WSP electrolysis process takes advantage of the reducing potential SO_2 to lower the electrolyzer voltage and produce H_2 using less higher-cost electrical energy.

4.2 Decomposition Reactor Operation

One mode of operation for the decomposition reactor is to use a shell-and-tube heat exchanger, fabricated from a high-temperature, corrosion resistant alloy. Hot helium or molten

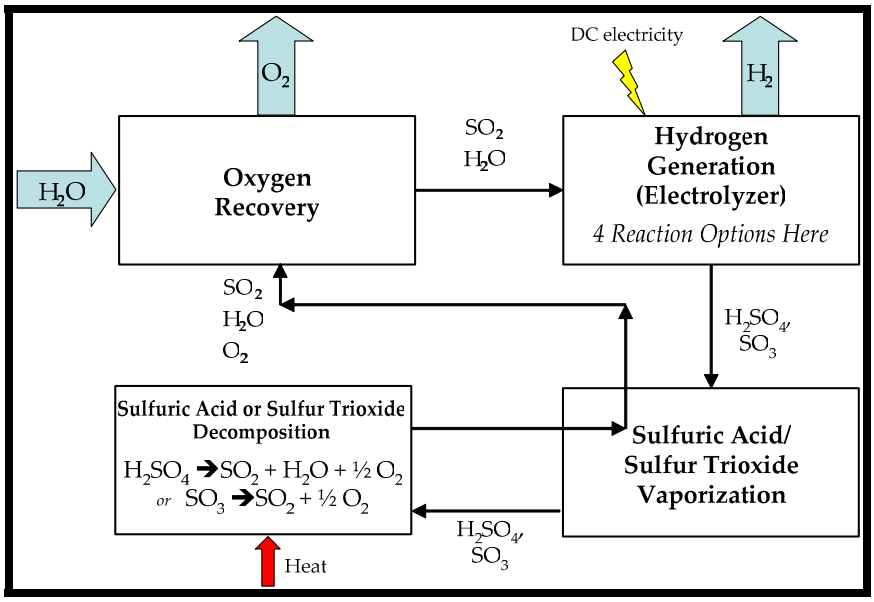

Figure 8 - Westinghouse Sulfur Process Block Diagram

salt IHX heat exchange fluid would flow on the shell side, with sulfur trioxide or H_2SO_4 on the tube side. The tubes would be packed with catalyst beads to increase the rate of the SO_3 decomposition reaction. The design must be robust, demanding pressure differentials of up to 10.1 MPa and temperature differentials up to 900°C. Alternatively, the decomposition reactor may be a directly heated bed of catalyst particles,[6] which simplifies construction and design at the cost of a somewhat more complex semibatch operation.

There are two options for the reaction in the decomposition reactor. One uses sulfuric acid (or equivalently, sulfur trioxide hydrate) and the other uses anhydrous sulfur trioxide, with decomposition reactions as follows:

$$H_2SO_4 \rightarrow H_2O + SO_2 + ½ O_2 \quad (1)$$

$$SO_3 \rightarrow SO_2 + ½ O_2 \quad (2)$$

There are several advantages to choosing SO_3 over H_2SO_4 with regards to the decomposition reactor. Use of sulfuric acid creates greater corrosion issues in all portions of the process including the evaporation, reaction, and condensation, whereas lower alloy and therefore less expensive materials may be used if little or no water is present. In addition, using anhydrous sulfur trioxide minimizes the heat duty necessary to vaporize the feed materials. The decomposition reactor catalyst life is also much larger (at least five times greater as discussed below) when sulfur trioxide is used than with sulfuric acid. As discussed below, a disadvantage is that a higher voltage will be needed to be applied in the electrolyzer.

4.3 Oxygen Separation

After the decomposition unit, the oxygen is removed from the stream. As discussed in below, electrolysis can be accomplished with either liquid or vapor-phase SO_2 oxidation on one side of a membrane cell and with either steam or liquid water on the other side. All four of

these phase options were evaluated in the current study (Liquid-Aqueous, Liquid-Liquid, Gas-Gas, and Liquid-Gas, where the first term refers to the water phase, and the second to the sulfur species); each process has implications on the technology used for O_2-SO_x separation.

If electrolysis is done using aqueous phase H_2SO_4, (the design basis for which the most experimental data are available), O_2 removal may be accomplished by first cooling the hot SO_x-O_2 mixture and then scrubbing it with the makeup H_2O shown in Figure 8. Sulfur dioxide is dissolved to form sulfurous acid, creating the electrolysis reactor feed; undissociated SO_3 is also hydrolyzed to regenerate a sulfuric acid background. An improvement over the original Westinghouse sulfur process is to increase the pressure of the scrubbing/absorption step, minimizing the amount of water required (which must later to evaporated in the decomposition reactor).

Further increase in the pressure will result in condensation of the recycled SO_2 to a liquid, at which point the water requirement is limited to only that needed for electrolysis feed, plus whatever small quantity dissolves in the liquid SO_2. The electrolyzer feed in this case is actually a two-phase liquid.[7] Oxygen is minimally absorbed by the scrubber water, and is separated by phase disengagement. The primary energy usage in this case is the heat rejection to the cooling water needed to condense the hot SO_x mixture leaving the decomposition reactor. Note that CHEMCAD modeling of this system is believed to be the least reliable, due to questions about the reliability of solubility and phase equilibrium data in high pressure liquid SO_2.

If a gas-phase separation of O_2 from SO_x is employed (either the Liquid-Gas or Gas-Gas configurations), the entire process loop becomes gaseous, and the need to vaporize either water or SO_3 is eliminated from the flowsheet. However, the separation process may be energy-intensive. The currently modeled process assumes semibatch absorption of SO_x onto zeolite columns at 80°C, where a column capacity of 0.26 kg SO_2 per kg of absorbent has been used. When the column is fully loaded, absorption is switched to another column, and hot O_2-SO_x mixture is routed to the saturated column to heat it to 300°C and desorb the oxygen. The small amount of oxygen contamination of the electrolyzer feed is not expected to have a major impact on its performance. However, the heat duty needed to bring the column packing from 80°C to 300°C is substantial, and amounts to 35 to 45% of the entire thermal IHX energy. This demand severely penalizes both the Liquid-Gas and Gas-Gas processes, and points to the need to evaluate other gas-phase separation technologies such as low-temperature membrane separation.

4.4 Electrolysis

The four different options each imply different reactions within the electrolyzer, as follows:[8]

$$2\ H_2O\ (\ell) + SO_2\ (aq) \rightarrow H_2\ (g) + H_2SO_4\ (aq)\ ; \quad \Delta G^\circ_{React} = 30.4\ \text{kJ/mol}; \quad \mathbf{E}^\circ = 0.16\ \text{V} \qquad (3)$$

$$H_2O\ (\ell) + SO_2\ (\ell) \rightarrow H_2\ (g) + SO_3\ (\ell)\ ; \quad \Delta G^\circ_{React} = 163.6\ \text{kJ/mol} \quad \mathbf{E}^\circ = 0.85\ \text{V} \qquad (4)$$

$$H_2O\ (g) + SO_2\ (g) \rightarrow H_2\ (g) + SO_3\ (g)\ ; \quad \Delta G^\circ_{React} = 157.7\ \text{kJ/mol} \quad \mathbf{E}^\circ = 0.82\ \text{V} \qquad (5)$$

$H_2O\ (\ell) + SO_2\ (g) \rightarrow H_2\ (g) + SO_3\ (g)$; ΔG°_{React} = 166.3 kJ/mol **E**° = 0.86 V (6)

The first reaction describes the original Westinghouse Sulfur Process, operating at 50°C and roughly 0.57 V with noble metal electrodes to avoid sulfuric acid corrosion. It is notable that the theoretical voltage **E**° for Reaction (3) as computed from Faraday's equation

$$-\Delta G^\circ_{React} = n\ \mathbf{F}\ \mathbf{E}^\circ\ , \qquad (7)$$

is equal to only 0.16 volts (n = 2 and **F** = 96,500 coulombs). Substantial cell losses of about 0.4 volts are therefore observed, increasing the actual electrical power consumption by a factor of β = (0.16+0.4)/0.16 = 3.50 over theoretical for Reaction (3). The observed actual free energy is therefore equal to $\Delta G_{Act} = \beta\, \Delta G^\circ_{React}$.

Westinghouse has proposed a fundamental improvement over the original process, involving raising the pressure to increase the solubility of SO_2 in the aqueous feed as well as provide for SO_2 condensation as a liquid below its critical point of 157.5°C and 7.8 MPa. Elimination of most of the water in the Liquid-Liquid option described by Reaction (4), and supplying only what is needed by the electrolytic reaction further positively impacts overall efficiency by minimizing vaporization heat duty for circulating water. However (as indicated above), it also requires significantly higher theoretical cell voltages. Assuming the same 0.4 voltage loss (since all four electrolyzers involve proton transfer membranes, and therefore are expected to suffer roughly the same overvoltage loss), the actual electrical power consumption would exceed the theoretical by a factor of β = (0.85+0.4)/0.85 = 1.47. The pressure has also been increased from atmospheric pressure to 10 MPa to accomplish condensation of the SO_2 without excess water to dissolve it.

As shown in Table 6, the decreased vaporization duty reduces the thermal megawatts K (MJ/kg H_2) required from (for example, at 900°C primary He temperature with a He loop) K = 110.5 for the Liquid-Aqueous system to 73.9 for the Liquid-Liquid system. At the same time, the electrolytic energy requirement (ΔG_{Act} = theoretical plus overvoltage) increases from 54.9 to 134.5 MJ/kg. The circulating SO_x consists of 99% SO_3, as compared to 50% H_2SO_4 (41% SO_3 equivalent) in the Liquid-Aqueous model. The heat provided to the decomposition reactor is thus used more efficiently (none is consumed evaporating and heating water), although at elevated pressure Le Chatelier's Principle decreases the decomposition efficiency (33% for high-pressure SO_3 as compared to 95% for aqueous H_2SO_4). The circulation rate of the recycle SO_3 increases to accommodate the heat duty by greater throughput (almost 200 kg/s SO_3, as compared to 94 kg/s of recirculated aqueous H_2SO_4). The improvements in production rate and efficiency are at the cost of higher pressure equipment design and manufacture, plus increased SO_x circulation costs (which have not been estimated in the current model).

Note that Table 6 also indicates that use of molten salts as the heat transfer medium does reduce the energy requirements per unit hydrogen production. The improvement in thermal energy demand is small; most of the benefit comes from electrical usage, since liquid pumping is much more efficient than gas compression. Note that modeling of the molten salt

Table 6 – Comparative Energy Consumption for Hydrogen Production by Sulfur Cycles

Primary He Inlet Temperature to IHX (°C)	Sulfur Cycle (H_2O - SO_x)	MWt Consumed by WSP per Unit H_2 Production Rate (K; MJ/kg H_2)		MWe Consumed by WSP per Unit H_2 Production Rate (ΔG_{Act}; MJ/kg H_2)	
		He	MS	He	MS
900	Liquid-Aqueous	110.5	110.3	54.9	53.2
	Liquid-Liquid	73.9	---	134.5	---
	Gas-Gas	108.7	108.0	124.0	121.0
	Liquid-Gas	88.0	87.5	125.0	123.1
950	Liquid-Aqueous	112.4	---	55.1	---
	Liquid-Liquid	69.1	---	112.0	---
	Gas-Gas	103.2	---	123.5	---
	Liquid-Gas	82.4	81.9	123.1	122.7

systems is currently incomplete, so that some data are absent from the table.

Reaction (5) involves completely gas phase electrolysis of the SO_2 to SO_3 using available technology.[9] In this process, steam and hydrogen are used on one side of a hydrated membrane such as Nafion, while SO_2 gas is exposed to the other. A high enough current flow is induced over the membrane to make water diffusion across the membrane bethe limiting step such that not all of the SO_2 is converted to SO_3. A vaporizer is required to convert makeup feed water to steam before injecting into the electrolyzer. The reaction pressure is nominally atmospheric in the current simulation, so that the electrolysis temperature is slightly above 100°C (higher temperatures would lead to more rapid membrane degradation). Actual to theoretical power consumption would be β = 1.47 assuming 0.4 volts loss. Note that laboratory experimental data[10] show cell operation at 1.1 to 1.2 volts, a loss of only 0.28 to 0.38 volts (β = 1.34 to 1.46), so that use of a value of β = 1.50 ratio may be somewhat conservative.

As shown in Table 6, the increased heat duty required to evaporate the incoming water feed significantly increases the thermal heat duty per kg H_2 generated, increasing from 69.2 MJ/kg for Liquid-Liquid up to 103.2 for Gas-Gas in the 950°C case. Part of this penalty is also related to the heat duty required to desorb SO_x from the zeolite column. Since the theoretical voltage is roughly the same as the Liquid-Liquid system, the computed electrical consumption is comparable. Operation at the higher voltage levels required for gas-phase SO_3 electrolysis results in a smaller electrolysis unit due to the very high current densities achieved.

Note that once again, the current model has not attempted to take into account circulation losses in the sulfur process. As shown in Table 7, circulation requirements for the Liquid-Aqueous and Liquid-Liquid processes pump liquids only, with flowrates ranging from 100 to 200 kg/s. For the Gas-Gas process, however, the recirculation stream consists of a gas-phase SO_3-O_2 mixture at flowrates of 40-100 kg/s. This circulation duty will thus require a large compressor, with associated much larger capital cost and electrical motor requirements.

An additional issue with the Gas-Gas process is the size and efficiency of the heat

Table 7 – Circulation Requirements in the Four Sulfur Cycles

Sulfur Cycle (H_2O - SO_x)	Pressure (MPa)	Heat Extracted by IXH (MWt)	Recycle Rate (kg/s)*		Recycle Stream Composition
			T(He)= 900°C	T(He)= 950°C	
Liquid-Aqueous	5.0	50	43	46	50% wt H_2SO_4-50%wt H_2O Liquid
		100	86	94	
		150	131	144	
Liquid-Liquid	10.0	50	83	104	98% SO_3-1.5% SO_2-0.5% O_2 Liquid
		100	159	194	
		150	134	216	
Gas-Gas	0.1	50	34	40	73% SO_3-2% SO_2-25% O_2 Gas
		100	66	74	
		150	100	113	
Liquid-Gas	0.1	50	43	49	73% SO_3-2% SO_2-25% O_2 Gas
		100	82	91	
		150	125	137	

*As evaluated He heat transfer loop; SO_x recycle rates are 1.5 to 3.5% greater for molten salts.

Table 8 – Decomposition Reactor, Preheat, and Desorption Duties for the Four Sulfur Cycles

Sulfur Cycle (H_2O - SO_x)	Heat Extracted by IXH (MWt)	Decomposition Reactor Duty (MWt)		Reactor Preheat Duty (MWt)		SO_x-O_2 Separator Desorption Duty (MWt)	
		He	MS	He	MS	He	MS
Liquid-Aqueous	50	45.6	---	108.6	---	n/a	
	100	93.4	96.5	222.6	228.5		
	150	142.4	145.1	339.3	343.7		
Liquid-Liquid	50	49.4	---	77.1	---	n/a	
	100	92.9	---	143.8	---		
	150	102.4	---	160.1	---		
Gas-Gas	50	40.4	---	6.6	---	17.8	---
	100	75.4	---	12.8	---	33.6	---
	150	114.7	116.7	19.5	---	51.1	52.0
Liquid-Gas	50	49.7	47.3	8.3	8.0	22.2	21.1
	100	93.3	95.9	15.3	16.3	41.3	42.8
	150	141.8	144.1	23.7	24.5	62.9	64.3

exchangers involved. In all cases, the hot fluid exiting the decomposition reactor is used to preheat the reactor feed. As shown in Table 8, heat exchange duties are on the order of 150 to 200 MW, which will require very large heat exchange surface area. For the Liquid-Liquid and Liquid-Aqueous systems, operating with a liquid phase on one side of the exchanger will improve heat exchange coefficients and reduce the area requirement somewhat. This benefit is not available for the Gas-Gas system, leading to larger equipment sizes and capital costs.

A fourth mode of operation is to use liquid water rather than steam, with gas phase SO_2 on the other side of the membrane. The chemistry is shown in Reaction (6), with an expected actual-to-theoretical ratio of β=1.49. While operation of this process results in an energy penalty due to a slightly higher voltage as compared to the gas-gas configuration, this penalty is off-set by the elimination of the need to vaporize water. As seen in Table 6, the thermal requirement is intermediate between those of the Liquid-Liquid and Gas-Gas configurations, while the electrical requirement differs little from that of the Gas-Gas system.

As in the case of the Liquid-Liquid and Gas-Gas designs, the absence or near-absence of water vapor in the flow to the decomposition reactor is expected to greatly extend the life of the decomposition catalyst. Catalyst life was determined not to be an issue when SO_3 was the sole feed component to the catalyst (>1,000 hours).[10] However, recent tests that use H_2SO_4 as the feed (H_2O plus SO_3) have much shorter catalyst lives (~200 hours).[11] Additional testing would be required to determine the carryover of water from the three nominally dry electrolysis reactors, and the effect of this water vapor on decomposition reactor catalyst life.

4.5 Efficiency Comparison of Four Sulfur Cycle Models

In comparing the relative efficiencies of the four sulfur cycle processes, the following efficiency $\eta(H_2)$ has been defined, the ratio of the thermal power which can be extracted from the H_2 generated, divided by the sum of the thermal power delivered to the WSP plus the thermal power equivalent of the electrical power consumed by the WSP:

$$\eta(H_2) = \frac{(\Delta H_{LHV}; MJ/kg)(M_{H2}; kg/s)}{(Q_{IHX}; MWt) + (\Sigma E; MWe)/0.38} \quad (8)$$

Here, M_{H2} is the hydrogen generation rate, ΔH_{LHV} is the lower heating value of the hydrogen (120 MJ/kg), Q_{IHX} the power delivered by the intermediate heat exchange loop, ΣE is the sum of electrical requirements for the WSP (electrolysis plus circulation), and 0.38 is the assumed electrical-to-thermal efficiency of the electrical power input.

The basis of the material and energy balances assumes that each of the heat exchangers will operation no closer than 50°C to pinch, to minimize the size of the already very large heat exchangers. Therefore, for a primary helium temperature of 900°C, the IHX helium or molten salt exit temperature from the IHX will be 850°C, losing only a few degrees in the supply line of the intermediate heat exchanger. The same pinch constraint will then apply to the decomposition reactor, so that the exit SO_x stream leaving the DR will be approximately 800°C. To avoid pinching on the other side of the IHX, the return He or MS temperature (T_R) must be 50°C below the primary helium exit temperature T_X, which in turn depends on the total

IHX power extracted from the primary He loop. The control logic of the model adjusts the flowrate of SO_x entering the decomposition reactor until its heat duty Q_{DR} is such that the value of T_R is equal to the specified value satisfying the pinch constraints.

Thus, for a specified primary He temperature and IHX power extraction, the circulating SO_x flowrate is fixed, which further establishes the production rate of hydrogen from the cycle. M_{H2} is therefore directly proportional to Q_{DR}, the power delivered to the decomposition reactor. For sulfur cycles involving aqueous H_2SO_4 or the Liquid-Liquid option, Q_{DR} is nearly equal to Q_{IHX}, the only other thermal loss (3-5%) being preheating of the incoming makeup water to electrolysis reactor temperature (90°C). In the case of the Liquid-Gas cycle, the process suffers the penalty discussed above for thermal desorption of the SO_x-saturated zeolite, so that only about 54% of the process heat is available for SO_3 decomposition. Finally, in the Gas-Gas case, water must also be vaporized at atmospheric pressure, consuming an additional ~21% of the available thermal power in the IHX, and leaving only 24% for SO_3 decomposition.

Overall energy efficiencies as defined above are shown in Table 9. These calculations were performed with a PCU operating at 38% efficiency and a molten salt or He high temperature heat transfer loop. Efficiencies are seen to insensitive to the heat extraction in the IHX; substitution of MS for He heat transfer loop fluid has a minor impact. The Liquid-Aqueous process (the sulfuric acid based process) has the highest efficiency at about 47%. The next highest process, the Liquid-Liquid process, is observed to have an $\eta(H_2)$ equal to 28% at the lower reactor He delivery temperature of 900°C increasing to 33% as the temperature is increased to 950°C. The Gas-Gas process also exhibits an efficiency of about 28%, increasing incrementally at higher reactor temperature, while the Liquid-Liquid process is essentially constant at 29%. It is important to note that these last two processes both suffer severe penalties from the heat of desorption of the zeolite absorbers, however; replacement of this technology by a less energy-intensive separation such as membranes would be expected to improve both efficiencies by about 2% points to a maximum of ~31%.

The main issue with all of the alternate processes to the sulfuric acid approach is that electrical energy which has a multiplier of 2.6 on conversion to thermal energy is substituted for thermal. That is, as the voltage for the electrolysis hydrogen production portion increases by about a factor of 2, the substitution of electrical for thermal severely penalizes the overall efficiency of the hydrogen generation process.

4.6 Estimate of Hydrogen Generation Costs

The throughput for the WSP-PBMR-PCU was determined using the energy use data derived above. The parameters that were used were:

1. K value of 110.5 MJ/kg H_2 for sulfuric acid based Liquid-Aqueous WSP (see Table 6)
2. ΔG_{Act} value of 54.9 MJ/kg H_2 for the sulfuric acid based WSP (see Table 6)
3. P_{PBMR} value was set at 577.3 MW for the high pressure nominal 600 MW Rankine cycle operating at 900°C (see Table 3)
4. Power conversion efficiency of 38%.

Table 9 – Overall Energy Efficiencies for the Four Sulfur Cycles

Sulfur Cycle (H_2O - SO_x)	Heat Extracted by IXH (MWt)	Overall Efficiency $\eta(H_2)$			
		T(Primary He) = 900°C		T(Primary He) = 950°C	
		He	MS	He	MS
Liquid-Aqueous	50	47.1%	---	47.0%	---
	100	47.4%	47.7%	46.6%	---
	150	47.3%	48.0%	46.7%	---
Liquid-Liquid	50	27.3%	---	32.3%	---
	100	28.1%	---	33.3%	---
	150	28.7%	---	33.4%	---
Gas-Gas	50	26.3%	---	27.3%	---
	100	28.0%	---	28.4%	---
	150	28.0%	28.1%	28.4%	---
Liquid-Gas	50	27.6%	29.0%	---	29.4%
	100	28.9%	29.1%	29.4%	29.6%
	150	29.0%	29.2%	---	29.7%

An energy balance around the process gives:

PBMR Thermal Power = Electrical Power + Thermal Power to the IHX

P_{PBMR} = (Q_{IHX} / K) (ΔG_{Act} / 0.38) + Q_{IHX} ;
577.3 = (Q_{IHX} / 110.5) (54.9 / 0.38) + Q_{IHX}

Solving for Q_{IHX} gives 250.2 MWt. For a K value of 110.5 MJ/kg H_2, this gives a plant hydrogen production rate of 2.26 kg/s, or 8,151 kg H_2/hr.

The energy cost for hydrogen was then calculated using Equation (9):

$$\alpha_{Hydrogen} = \frac{\alpha_{Thermal} \cdot K + \alpha_{Electrical} \cdot \Delta G_{Act}}{3600 \cdot \sec} \quad (9)$$

Note that one option that has been considered is to operate two PBMR's, one dedicated to providing the WSP thermal power and the second producing electricity. The above numbers do not take into account the increased energy efficiency and likely lower capital cost of using two separate PBMR's. In this case, the electrical PBMR would generate energy at a higher efficiency (about 43% using a Brayton cycle) and the second would generate thermal energy only thereby eliminating many of the current components from the loop.

The capital cost of the WSP was estimated by assuming that the capital cost of this plant would be roughly the same as that of an electrolytic chlor-alkali plant, corrected of course for current densities on the electrodes and the molecular weight of the products. In this approach, we assume that the electrolysis cell costs are directly transferable from chlorine to

hydrogen, while the feed and alkali processing cost portions of the plant approximately equal those of the decomposition reactor, absorber and other chemical processing sections of the WSP. Table 10 provides the factors that were used to scale between the chlor-alkali plant and the WSP. The first corrects for the difference in molecular weight and the difference in current densities:

$$H_2 \text{ Capacity} \approx Cl_2 \text{ Capacity} \times (2/70.9) \times (200/69) = 0.082 \times Cl_2 \text{ Capacity (tons/yr)}$$

The data for this analysis are shown in the first four columns of Table 11. These data are corrected back to U.S. 2003 prices using the Guthrie country correction[12] and the Chemical Engineering magazine yearly cost correction,[13] and are shown in column 7 of the table. The correction factors from chlorine to hydrogen capacity are applied in the next to column to obtain the equivalent *M*, and the unit costs C are shown in the final column.

Table 10 – Scale Factors Between H_2 and Chlor-Alkali Plants

Parameter	Chlorine	Hydrogen
Molecular Weight (g/mol)	70.9	2.0
Theoretical Voltage (volts)	4.0	0.61
Current Density (mA/cm^2)	69	200
Ampere Efficiency (%)	97	97
Mass Ratio $Cl_2 \rightarrow H_2$	2 / 70.9 = 0.0284 kg H_2/kg Cl_2	
Current Density Ratio $Cl_2 \rightarrow H_2$	200 / 69 = 2.90 kg H_2/kg Cl_2	

Table 11 – Unit Cost Data for H_2 Plants Based on Chlor-Alkali Plant Data

Estimated Cost ($million)	Capacity (tons Cl_2/day)	Year	Country	Ref	CE Year Correction	Guthrie Country Correction	Adjusted 2003 Cost ($million)	Equivalent H_2 Capacity *M* (kg/h)	Unit Capital Cost *C* [$k (kg/hr)$^{-1}$]
6	18	1980	Norway	14	261	0.86	10.7	55	193
24	60	1978	Argentina	14	219	1.06	41.4	184	224
30	80	1979	U.K.	14	239	0.89	56.4	246	229
43	300	1980	Turkey	14	261	1.10	59.9	922	65
50	375	1979	Japan	14	239	0.95	88.1	1153	76
26	400	1976	U.K.	14	192	0.89	60.9	1230	49
35	500	1974	Netherlands	14	165	0.98	86.6	1537	56
130	600	1981	Brazil	14	297	1.10	159.2	1845	86
110	750	1983	Netherlands	14	317	0.96	144.6	2306	63
81	1000	1980	Canada	14	261	1.05	118.2	3075	38
100	1500	1980	U.S.	14	261	1.00	156.3	4612	33
360	1205	2004	U.S.	14	400	1.00	360.0	3706	97
150	356	2003	Norway	15	400	1.00*	150.0	1095	137
55	52	2001	Australia	16	380	1.00*	57.9	161	359
213	1281	2003	U.S.	17	400	1.00*	212.5	3938	54

- Cost estimate already in U. S. dollars.

The logarithms of the unit cost C in \$k (kg H_2/hr)$^{-1}$ and H_2 capacity data M (kg H_2/hr) were regressed and the following cost equation generated ($r^2 = 0.75$):

$$\log_{10}(C) = 3.644 - 0.5545 \log_{10}(M) \; . \qquad (10)$$

The fit for these data is shown in Figure 9, where regression fits based on plant capacity are plotted against actual estimated costs from Table 11. Equation (10) was then used to estimate the capital and operating and maintenance costs for the WSP H_2 generation plant. The capital and O&M annual costs are estimated using the assumptions in Table 12. Using the electrical and thermal use estimates from Table 6 and combining with the unit cost for thermal and electrical energy in Equation (9), the unit cost of H_2 using a sulfuric acid based WSP was then determined to be (see Table 12) about \$1.67/kg H_2.

Table 12 – Unit Cost Estimate for H_2 Using the Sulfuric Acid Based WSP

Plant Size	8,151 kg/hr H_2
Estimated Unit Capital Cost	\$29,850 /(kg/hr H_2)
Availability	95%
Capital Charge (10 years)	17% /yr
Capital Cost Contribution	\$0.610 /kg H_2
Maintenance Charge Rate	10% of capital cost
Maintenance Cost Contribution	\$0.061 /kg H_2
Electrical Use	54.0 MWe/(kg/s H_2)
Thermal Use	110.5 MWt/(kg/s H_2)
Unit Electrical Cost	\$35 /MWh(e)
Unit Thermal Cost	\$15 /MWh(t)
Energy Costs	\$0.994 /kg H_2
Total Production Cost	\$1.67 /kg H_2

5. References

1. CHEMCAD Chemical Process Simulation software, V. 5.5.0, Chemstations Inc., Houston TX, July 12, 2005 release.
2. Greyvenstein, R., PBMR (Pty) Ltd., "*RE: Brayton Cycle (recuperator pressure drop)*," E-mail to the Author (EJL), June 24, 2005.
3. Greyvenstein, R., PBMR (Pty) Ltd., "*Feedback from Teleconference*," E-mail to the Author, June 28, 2005.
4. Matzner, D., "*PBMR Project Status and the Way Ahead*," September 2004.
5. Goossen, J. E., Lahoda, E. J., Matzie, R. A., Paoletti, L. A., and Task, K. D., "*Interfacing the Pebble Bed Modular Reactor with the Westinghouse Sulfur Process*," Am. Nucl. Soc. Annual Meeting, June 7, 2005.
6. Lahoda, E. J., Goossen, J. E., Matzie, R. A., and Mazzoccoli, J. P., "*Optimization of the Westinghouse Sulfur Process for Hydrogen Generation and the Interface with an HTGR*," Proc. 12th Intl. Conf. Nucl. Energy, Arlington VA, April, 2004.
7. Lahoda, E. J., Westinghouse Electric Company, "*Multiple Phase SO_3/SO_2/H_2O/H_2SO_4 Electrolyzer*," Patent Disclosure RDM-05-001, Pittsburgh PA, April, 2005.

8. Wagman, D. D., Evans, W. H., Parker, V. B., Schumm, R. H., Halow, I., Bailey, S. M., Churney, K. L., and Nuttall, R. L., "*The NBS Tables of Chemical Thermodynamic Properties*," J. Phys. Chem. Ref. Data, 11, Suppl. 2., 1982.
9. Sivasubramanian, P., Ramasamy, R. P., Holland. C. E., Weidner, J. W., and Freire, F. J., "*Electrochemical Generation of Hydrogen via Thermochemical Cycles*," AIChE Spring Meeting, Atlanta, April 2005.
10. Spewock, S., Brecher, L. E., and Talko, F., Proc. 1st World Hydrogen Energy Conf., V.3, 1976.
11. Ginosar, D. M., Glenn, A. W., and Petkovic, L. M., "*Stability of Sulfuric Acid Decomposition Catalysts for Thermochemical Water Splitting Cycles*," AIChE Spring Meeting, Atlanta, April 2005.
12. Guthrie, K. M., Process Plant Estimating Evaluation and Control, Craftsman Book Co., Carlsbad CA, 1974.
13. "*Chemical Engineering Plant Cost Index (CEPCI)*," Chem. Eng.; Available online at www.che.com.
14. Kharbanda, O. P., "*Capital Estimation Based on Chlorine Plants*," in Process Plant and Equipment Cost Estimation, Craftsman Book Co., Carlsbad CA, 1979.
15. Board of Norsk Hydro, Oslo, Norway, Press release, March 18, 2003.
16. Sterling Chemicals Holdings Inc., Houston TX, Press release, January 24, 2001 (60,000 metric tonnes/yr sodium chlorate).
17. "*Caustic Soda Chemical Profile*," The Innovation Group, Morristown NJ; available online at www.the-innovation-group.com/ChemProfiles/Caustic%20Soda.htm.